Int. J. Solids Structures, 1973, Vol. 9, pp. 951 to 965. Pergamon Press. Printed in Great Britain

ELASTIC BEHAVIOR, BRITTLE FAILURE AND PLASTIC FLOW OF FILAMENTARY MATERIALS

P. V. McLAUGHLIN, JR.,† S. MAJUMDAR‡ and J. W. PHILLIPS§

Department of Theoretical and Applied Mechanics,
University of Illinois at Urbana-Champaign, Urbana, Illinois 61801, U.S.A.

Abstract—The general features of elastic behavior, brittle failure, and plastic yielding are investigated under plane stress for a material composed of arrays of elastic–brittle or elastic–plastic filaments. Filamentary material linear elastic constitutive relations are derived and conditions for planar elastic isotropy are explored. Initial and subsequent fracture surfaces (which are generally anisotropic) and stress–strain behavior are computed for brittle filament materials. The form of incremental plastic stress–strain laws, initial yield surfaces, and subsequent yield surfaces are presented for general filament work-hardening. Examples are presented for brittle, perfectly plastic, and kinematic linear work hardening filaments, illustrating application of the analysis and the main results.

INTRODUCTION

THE PRESENT paper deals with the plane stress elastic behavior, brittle failure, and plastic behavior of a class of filamentary materials which are composed of a planar array of long elastic–brittle or elastic–plastic filaments. There are three general situations to which this study would directly apply:

(1) Materials made up of filaments alone without any significant matrix, e.g. paper, plastic and wire screens, woven and nonwoven textiles, sintered random wire filter media, etc.

(2) Wrapped reinforcement for weak structures where the reinforcement is not bonded to the structure and acts independently therefrom. Examples are steel wrapped hydraulic hoses and polymeric filament mesh reinforcing for air structures.

(3) Composite materials consisting of a relatively weak matrix reinforced by high strength filaments. Contribution of the matrix to the overall stiffness or the strength of the composite in the direction of reinforcement is generally small compared to that of the filaments [1].¶ Composites with three or more noncoincident families of reinforcement are therefore generally controlled by filament behavior [2, 3].

The assumption of essentially continuous filaments renders the present analysis inapplicable to the very important and critical case of short high strength brittle fibers in a matrix. The section on brittle failure, however, does apply to long, brittle filamentary arrays with no matrix as described in situations (1) and (2) above, or long, brittle filaments in a weak matrix where material behavior, fiber-matrix load characteristics, and/or

† Assistant Professor, currently, Senior Engineer, Materials Sciences Corp., Bluebell, PA. 19422, U.S.A.
‡ Research Assistant.
§ Assistant Professor.
¶ Numbers in square brackets denote references at the end of the paper.

loading conditions do not cause filament fracture from buildup of axial force due to matrix shear stresses.

Limit behavior and maximum plastic strength of filamentary materials when filaments are perfectly plastic have been investigated by McLaughlin and Batterman [2] for no matrix and by McLaughlin [3] when a matrix of significant strength surrounds the filaments. Behavior of general hyperelastic fiber network structures has been given by Wozniak [4], but no attention has been given to initial yield, subsequent yield, or brittle fracture of these materials. In the present paper, the salient features of filamentary materials having three or more filament families are exposed by considering the material's response to macroscopically uniform general plane stress and deformation. Elastic constitutive relations, brittle fracture properties, and plastic yield behavior (both initial and subsequent) are presented in terms of filament material properties and orientation geometry. In order to keep the analysis general, tensile behavior of the filaments is assumed brittle or work-hardening, but specific properties such as fracture or yield strengths in tension and compression, work-hardening law, etc. are kept unspecified. Specific examples which illustrate the main results of the analysis are presented for the simplest realistic models of filament behavior: elastic–brittle with equal properties in tension and compression, and elastic–linear kinematic work hardening with equal properties in tension and compression. The examples were performed by a computer program which calculates macroscopic filamentary material stresses and strains, and individual filament stresses and strains for desired loading or straining histories. In addition, the program computes and draws fracture and yield surfaces at successive stages of loading. The program is described in the Appendix.

BASIC ASSUMPTIONS, EQUILIBRIUM AND KINEMATIC CONSIDERATIONS

A representative structural element (RSE) of the filamentary material under consideration is shown in Fig. 1. The RSE is composed of many long, nearly straight filaments at various angles in a planar array. If there is a matrix material surrounding the filaments, its overall contribution to stiffness and strength of the total material is assumed to be of second order compared to the contribution of the filaments. Filaments may be interwoven, but the depth scale of the interweave is assumed small. Flexural behavior of the RSE is assumed negligible compared to membrane force effects. Since the main purpose of this study is determination of the response of the RSE under macroscopically plane stress conditions, we will ignore secondary effects such as couple stresses due to nonuniform filament spacing, or warping of the section because of nonsymmetrical filament family stacking sequences. Filament material behavior will be elastic–brittle and elastic–work hardening. Throughout the analysis, deformations will be assumed small so that no essential macroscopic geometry changes occur, although individual microscopic filament buckling is allowed.

Rectangular cartesian axes x_1 and x_2 are fixed in the center of the RSE, which is of unit dimensions. The ith family of filaments ($i = 1, 2, \ldots, m$) is spaced regularly at the rate of v_i filaments per unit length and is at an angle of θ_i to the x_1 axis. All filaments in a given family are assumed to have identical material and geometrical properties, although these properties may vary from one filament family to another.

Due to the geometrical and material regularity of each filament family, RSE macroscopic membrane forces per unit length $N_{\alpha\beta}$ ($\alpha, \beta = 1, 2$) will be homogeneous under a homogeneous macroscopic strain field, $\varepsilon_{\alpha\beta}$, and vice versa. The axial filament strain for

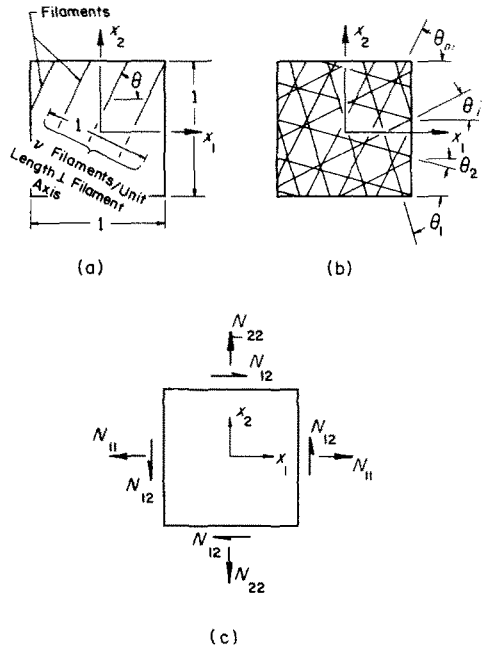

FIG. 1. Representative structural element of filamentary material. (a) Dimensions, filament orientation and number density. (b) Filament family numbering convention. (c) Macroscopic filamentary material stresses.

the ith filament family is given in terms of the macroscopic RSE strain by (summation convention for repeated Greek indices only)

$$e_i = \varepsilon_{\alpha\beta} n_\alpha^{(i)} n_\beta^{(i)} \tag{1}$$

where $n_x^{(i)}$ are the components of the unit vector along the axis of the ith fiber family,

$$n_1^{(i)} = \cos\theta_i \qquad n_2^{(i)} = \sin\theta_i$$

It will be assumed that the ith family filament stress, σ_i, is a known functional of the axial filament strain, e_i, denoted by

$$\sigma_i = \sigma_i(e_i). \tag{2}$$

The macroscopic membrane stress resultants may be written in terms of filament stress σ_i, number density ν_i, and filament cross-sectional area A_i, as

$$N_{\alpha\beta} = \sum_{i=1}^{m} \sigma_i A_i \nu_i n_\alpha^{(i)} n_\beta^{(i)}. \tag{3}$$

Note that the membrane stresses can, in principle, be easily found for any known membrane strain history by determining e_i from equation (1), computing the corresponding filament stresses from (2), then using equation (3). The inverse problem of finding membrane strains for a given membrane stress history will be straightforward only if the filament stress–axial strain relation (2) is a simple function, as occurs for elastic behavior. Complex functional constitutive laws such as plastic behavior will require numerical solution.

ELASTIC CONSTITUTIVE RELATIONS

In the case when all filaments behave linearly elastically, equation (2) may be written $\sigma_i = E_i e_i$, where E_i is the Young's Modulus for the ith filament family material. Used in conjunction with equations (1 and 3), this gives the macroscopic membrane stress–strain law

$$N_{\alpha\beta} = \sum_{i=1}^{m} E_i A_i v_i n_\alpha^{(i)} n_\beta^{(i)} n_\gamma^{(i)} n_\delta^{(i)} \varepsilon_{\gamma\delta} \tag{4a}$$

which may be written

$$N_{\alpha\beta} = C_{\alpha\beta\gamma\delta}\varepsilon_{\gamma\delta} \tag{4b}$$

where

$$C_{\alpha\beta\gamma\delta} = \sum_{i=1}^{m} E_i A_i v_i n_\alpha^{(i)} n_\beta^{(i)} n_\gamma^{(i)} n_\delta^{(i)}. \tag{4c}$$

Due to interchangeability of the four indices, there are only 5 independent components of $C_{\alpha\beta\gamma\delta}$. Equation (4b) may therefore be written in matrix form:

$$\begin{Bmatrix} N_{11} \\ N_{22} \\ N_{12} \end{Bmatrix} = \begin{bmatrix} C_{1111} & C_{1122} & C_{1112} \\ C_{1122} & C_{2222} & C_{1222} \\ C_{1112} & C_{1222} & C_{1122} \end{bmatrix} \begin{Bmatrix} \varepsilon_{11} \\ \varepsilon_{22} \\ 2\varepsilon_{12} \end{Bmatrix}. \tag{4d}$$

In the important case when filaments in all families have identical (E_i, v_i, A_i) properties, the membrane is elastically isotropic in-plane when composed of sets of equiangular arrays: Under an arbitrary planar counter–clockwise coordinate rotation ϕ, a membrane whose filaments are oriented equiangularly at $\theta_i = \alpha + \pi i/m$ has corresponding moduli (4c) equal to a set of constants plus linear combinations of

$$\sum_{i=1}^{m} \sin(2\theta_i + \phi), \quad \sum_{i=1}^{m} \cos(2\theta_i + \phi), \quad \sum_{i=1}^{m} \sin(4\theta_i + \phi) \quad \text{and} \quad \sum_{i=1}^{m} \cos(4\theta_i + \phi).$$

Since the sums

$$\sum_{i=1}^{m} \exp[2j(\theta_i + \phi)] = \exp\left\{2j\left[\phi + \left(\alpha + \frac{\pi}{m}\right)\right]\right\} \frac{1 - \exp(2\pi j)}{1 - \exp(2\pi j/m)} = 0 \quad \text{for } m \neq 1$$

and

$$\sum_{i=1}^{m} \exp[4j(\theta_i + \phi)] = \exp\left\{4j\left[\phi + \left(\alpha + \frac{\pi}{m}\right)\right]\right\} \frac{1 - \exp(4\pi j)}{1 - \exp(4\pi j/m)} = 0, \quad \text{for } m \neq 1 \text{ or } 2$$

where $j = \sqrt{-1}$, the sums of the trigonometric functions of $2\theta_i + \phi$ and $4\theta_i + \phi$ vanish for $m \geq 3$. Thus, a membrane with three or more equiangular filament families is elastically planar isotropic if filament family properties are identical. For this isotropic case, the moduli (4c) become

$$\begin{aligned} C_{1111} &= C_{2222} = 3EAvm/8 \\ C_{1122} &= EAvm/8 \\ C_{1112} &= C_{1222} = 0 \end{aligned} \tag{5}$$

where E and A are Young's Modulus and cross-sectional area of a typical filament, respectively, and v is the number density of each family. By superposition, a membrane composed of several sets of equiangular arrays at arbitrary relative orientation is also elastically planar isotropic. Typical isotropic arrays are shown in Fig. 2.

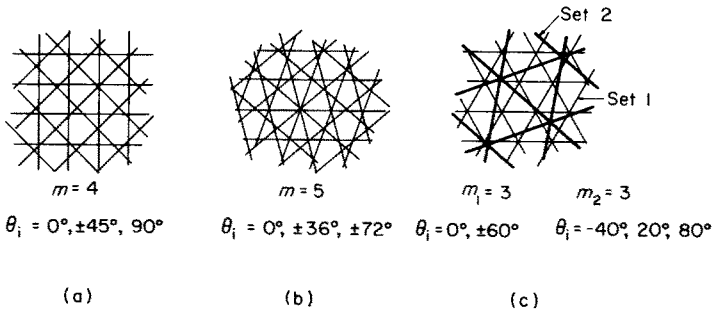

FIG. 2. Examples of elastically isotropic filament arrays. (a) and (b) Identical filament families. (c) Two unequal sets of families, each set with filaments identical within the set.

BRITTLE FAILURE

For filamentary materials which are elastic–brittle, the most common filament failure modes are brittle fracture in tension and elastic buckling or brittle fracture in compression. Let the filament tensile fracture stress and strain for the ith family be σ_i^t and $e_i^t = \sigma_i^t/E_i$, respectively, and the buckling or compressive fracture stress and strain be σ_i^c and $e_i^c = \sigma_i^c/E_i$, respectively. An initial failure surface in membrane stress space can be constructed which represents combinations of membrane stress causing filament fracture or buckling. For the kth family filaments at failure, from equations (1 and 4),

$$C^{-1}_{\alpha\beta\gamma\delta} N_{\gamma\delta} n_\alpha^{(k)} n_\beta^{(k)} = e_k^t, -e_k^c \tag{6}$$

where $C^{-1}_{\alpha\beta\gamma\delta}$ are the membrane elastic compliances obtained from inverting equation (5) to give $\varepsilon_{\alpha\beta} = C^{-1}_{\alpha\beta\gamma\delta} N_{\gamma\delta}$. It can be shown that a unique $C^{-1}_{\alpha\beta\gamma\delta}$ exists as long as $m \geq 3$. Equation (6) is the equation of two parallel planes (one each for e_k^t, e_k^c) in membrane stress space. The interior intersection of the 2-m planes as $k = 1 \rightarrow m$ is a closed surface in stress space and is the complete initial failure surface.

When all filament families have identical or nearly identical properties, the initial failure surface will be composed of 2-m planar surfaces. If filament family strength and/or stiffness properties are widely different in a given membrane, it is possible for the intersection of weaker family planes to be inside surfaces for the stronger families giving an initial failure surface composed of less than 2-m planar faces.

A large number of filamentary materials in current usage are composed of filament families with identical properties. For proportional stressing or straining of these materials, it can be shown that a further increase in membrane macroscopic stress is not possible once one family of filaments has fractured in tension. In addition, subsequent failure surfaces (computed by ignoring sequentially tensile–fractured filament families in equation (6)) lie inside previous surfaces except for a small range of loading combinations. Hence, for practical purposes, the initial fracture surface represents the maximum load carrying

capability of the membrane. Surfaces representing initial filament buckling (no fracture) will not, in general, be maximum stresses which can be borne by the material. Buckled filaments can still bear load after bifurcation and allow other filaments to achieve a higher stress under increasing applied load. This behavior is similar to perfect plasticity, and maximum stress envelopes can be computed by limit analysis [2, 5]. Only in the case of a three-family ($m = 3$) or less membrane with θ_i all different does the initial failure surface always represent combinations of maximum possible membrane stress regardless of failure mechanism. Fracture, buckling, or perfectly plastic flow of one filament family will leave at most two families which can deform as a mechanism and render further proportional increase in membrane stress impossible.

Typical initial and subsequent fracture behavior is illustrated for several filamentary materials in Fig. 3, where the n_{ij} are nondimensional macroscopic membrane stresses given by $n_{ij} = N_{ij}/\Sigma A_i v_i \sigma_i^f$. Figure 3a shows initial fracture surfaces for membranes composed of three, four and ten equiangularly oriented filament families with identical filament properties. In Fig. 3b, the effect of one filament fracturing on subsequent fracture surfaces of the $m = 4$ membrane is illustrated. The solid line shows the initial fracture surface, and the dashed lines show subsequent fracture surfaces that would be obtained after the

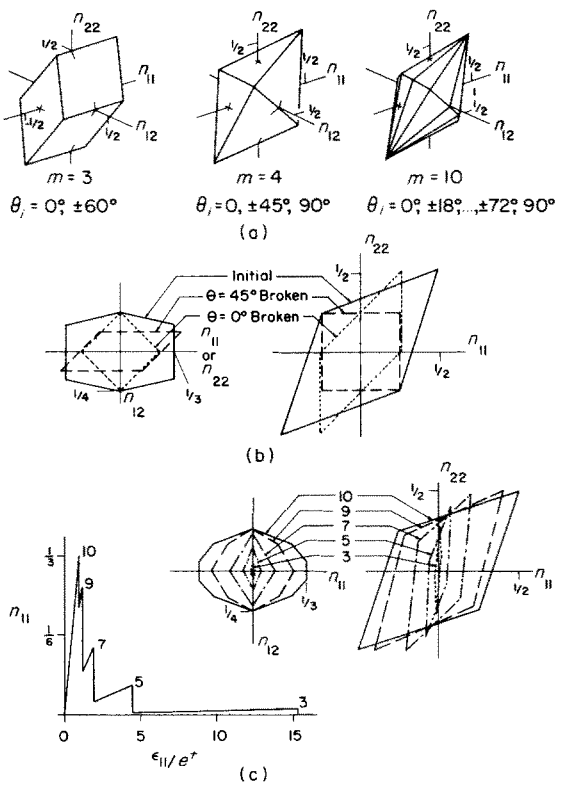

FIG. 3. Typical initial and subsequent fracture behavior of filamentary materials. $n_{ij} = N_{ij} \sum A_i v_i \sigma_i^f$. (a) Initial fracture surfaces. (b) Subsequent fracture surfaces, $m = 4$ ($\theta_i = 0, \pm 45, 90°$) material, for one filament family broken. (c) Subsequent fracture surfaces and stress–strain behavior for loading of $m = 10$ ($\theta_i = 0, \pm 18, \pm 36, \pm 54, \pm 72, 90°$) material in simple tension. Numbers indicate remaining (unbroken) filaments.

filaments at $+45$ or $0°$ break in tension due, for example, to pure shear (N_{12}) or axial force (N_{11}), respectively. Similar subsequent fracture surfaces occur if the filaments at $0 = -45$ or $+90°$ break.

Figure 3c shows initial and subsequent fracture behavior of a ten family membrane strained in uniaxial tension, ε_{11}. As the strain increases, filaments at $\theta = 0°$ fracture first giving a subsequent fracture surface indicated by the number 9. As straining progresses, filaments at $\theta = \pm 18°$ fracture leaving seven filaments, etc. Note from the stress–strain curve shown in Fig. 3c that the axial load never increases beyond the load at which the first filament family fractures. Also, in both Figs. 3b and c, subsequent fracture surfaces penetrate the initial fracture surface only in small regions far from the loading state which caused the filaments to fracture. It is noted that if the material is subjected to monotonic increasing membrane *stress*, brittle failure will be catastrophic upon reaching the initial failure surface, while for monotonic increasing membrane *strain*, the failure will be non-catastrophic except in the case of the three family filamentary material.

While equiangular arrays of identical filaments are elastically planar isotropic, the fracture behavior is highly anisotropic. All planar isotropic failure surfaces can in principle be written as a function of membrane plane stress invariants $N_{11}+N_{22}$ and $N_{11}N_{22}-N_{12}^2$ which may be expressed as follows:

$$f[(N_{11}+N_{22}), (N_{11}N_{22}-N_{12}^2)] = 0.$$

In principle, this equation can be solved to give $N_{11}N_{22}-N_{12}^2$ as a function of $N_{11}+N_{22}$:

$$N_{11}N_{22}-N_{12}^2 = g(N_{11}+N_{22}).$$

This may be rewritten

$$\tfrac{1}{4}(N_{22}-N_{11})^2+N_{12}^2 = -g(N_{11}+N_{22})+\tfrac{1}{4}(N_{11}+N_{22})^2 = k(N_{11}+N_{22}) \qquad (7)$$

which is a surface having an elliptical intersection with all planes $N_{11}+N_{22} =$ constant. The ratio of major to minor axes of the ellipse is always $\sqrt{2}$. The surface (7) is illustrated in Fig. 4a. Initial failure surfaces for all membranes with a finite number of filament families have plane surfaces and do not have the required elliptical cross-sections. Hence initial fracture behavior cannot be isotropic even if elastic behavior is.

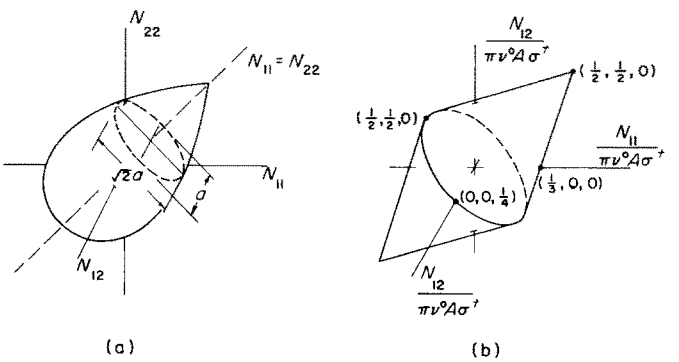

FIG. 4(a) Typical isotropic plane stress failure surface showing elliptical cross-section along $N_{11} = N_{22}$ axis. (b) Fracture surface for filamentary material with continuous uniform filament orientation ($m \to \infty$). $\nu°$ is number of filaments per unit angle θ.

Note from Fig. 3 that initial fracture behavior becomes closer to isotropic behavior as number of equiangular filament families increases, the three family membrane being least isotropic. If the number of filament families approaches infinity to cause the membrane to have uniform filament orientation in all directions, the resulting initial fracture behavior becomes isotropic. The initial fracture surface for uniform orientation is shown in Fig. 4b.

PLASTIC STRESS–STRAIN BEHAVIOR AND YIELD SURFACES

When filaments can sustain significant plastic flow before fracture as with metal wires or polymer strands, failure is normally considered to have occurred when plastic deformations become excessive and the maximum plastic load on the membrane is reached. Computations of the limit or plastic failure surface can be handled by use of limit analysis and has been performed in [2, 3]. To study initial and subsequent plastic behavior, filament plastic behavior is assumed to be of a very general work-hardening type (Fig. 5). Initial filament yielding occurs at stresses and strains of σ_i^{t0}, σ_i^{c0} and $e_i^{t0} = \sigma_i^{t0}/E_i$, $e_i^{c0} = \sigma_i^{c0}/E_i$ in tension and compression, respectively. The tangent modulus in tension and compression during yielding is denoted $E_i^T = \mathrm{d}\sigma_i/\mathrm{d}e_i$, and is in general a function of loading history. Likewise, the current values of filament yield stress in tension (σ_i^t) and compression (σ_i^c) are also functions of loading history.

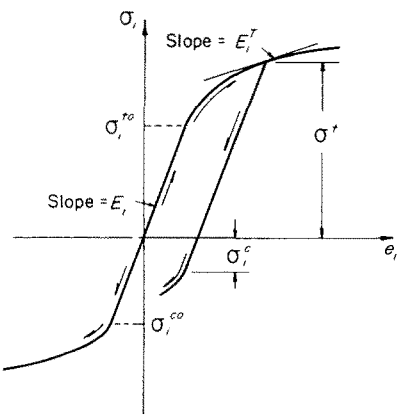

FIG. 5. Filament plastic behavior.

Initial yield

Initial yielding in a filamentary material occurs when the first family of filaments begins to yield. If the filaments are linearly elastic prior to yield, then equation (6) for brittle fracture or buckling will also give the initial yield surface if e_i^t and e_i^c are replaced by the initial axial yield strains, e_i^{t0} and e_i^{c0}. Hence, initial yield surfaces have the same properties as fracture surfaces. Note in particular that initial yield surfaces for finite numbers of filament families will be anisotropic even though elastic behavior is isotropic. Only in the case of uniform orientation of identical filaments will the initial yield behavior be isotropic.

Stress–strain relations in the plastic range

Because of the discontinuous nature of plastic stress–strain relations, it is convenient to write them in incremental or rate form. Let all increments or rates be denoted by an overdot. The axial strain increment of the ith filament family in terms of elastic (superscript e) and plastic (superscript p) strain increments is

$$\dot{e}_i = \dot{e}_i^e + \dot{e}_i^p \tag{8a}$$

where

$$\dot{e}_i^e = \dot{\sigma}_i / E_i \tag{8b}$$

$$\dot{e}_i^p = \begin{cases} \dot{\sigma}_i / E_i^T & \text{(plastic loading)} \\ 0 & \text{(elastic loading or unloading).} \end{cases} \tag{8c}$$

Equations (1 and 3) in incremental form may be combined with equations (8) to give the membrane incremental stress–strain relation or flow law

$$\dot{N}_{\alpha\beta} = \left[\sum_{i=1}^{m} E_i A_i v_i n_\alpha^{(i)} n_\beta^{(i)} n_\gamma^{(i)} n_\delta^{(i)} - \sum_{i=1}^{m}{}^{*} (E_i - E_i^T) A_i v_i n_\alpha^{(i)} n_\beta^{(i)} n_\gamma^{(i)} n_\delta^{(i)} \right] \dot{\varepsilon}_{\gamma\delta} \tag{9a}$$

$$= (C_{\alpha\beta\gamma\delta} - C^*_{\alpha\beta\gamma\delta}) \dot{\varepsilon}_{\gamma\delta} \tag{9b}$$

where $\sum^*$ denotes summing only over those i for which filaments are yielding and $\dot{e}_i^p \neq 0$. The $C_{\alpha\beta\gamma\delta}$ are the elastic moduli as before, and $C^*_{\alpha\beta\gamma\delta}$ are defined by the above equation. The flow law may be put into the usual inverse form

$$\dot{e}_{\alpha\beta} = C^{-1}_{\alpha\beta\gamma\delta} \dot{N}_{\gamma\delta} + D_{\alpha\beta\gamma\delta} \dot{N}_{\gamma\delta} \tag{9c}$$

where the first and second terms are the elastic and plastic components of the macroscopic membrane strains, respectively, $C^{-1}_{\alpha\beta\gamma\delta}$ are the elastic compliances as before, and $D_{\alpha\beta\gamma\delta}$ are the plastic compliances given by

$$D_{\alpha\beta\gamma\delta} = (C_{\alpha\beta\gamma\delta} - C^*_{\alpha\beta\gamma\delta})^{-1} - C^{-1}_{\alpha\beta\gamma\delta}. \tag{9d}$$

It can be shown that the inverse $(C_{\alpha\beta\gamma\delta} - C^*_{\alpha\beta\gamma\delta})^{-1}$ is unique for $m \geq 3$ and work-hardening filaments ($E_i^T \neq 0$). For perfectly plastic filaments ($E_i^T = 0$), a unique inverse exists as long as there are at least 3 unyielded filaments. It is noted that $C_{\alpha\beta\gamma\delta}$ and its inverse remain constant throughout stressing or straining of the membrane, while $C^*_{\alpha\beta\gamma\delta}$ and $D_{\alpha\beta\gamma\delta}$ depend on strain history and hence must be recalculated at each step of the loading. If no filament family yields in an increment of loading, $D_{\alpha\beta\gamma\delta}$ vanishes by definition of $C^*_{\alpha\beta\gamma\delta}$.

Subsequent yield surfaces

When a filamentary material is loaded past the point where the first filament family begins to yield, the yield surface, in general, changes shape and translates. The subsequent yield surface at any stage of loading past initial yield is defined to be the boundary of the locus of all points which may be reached under purely elastic behavior of all filaments. If at any stage of plastic loading beyond initial yield the current yield stresses and the axial stress of each filament family are known, then the subsequent yield surface may be computed as follows:

Let $N^l_{\alpha\beta}$ be the current plastic loading point (which by definition is on the subsequent yield surface) and $N^y_{\alpha\beta} = N^l_{\alpha\beta} + \Delta N_{\alpha\beta}$ be any other point on the subsequent yield surface.

Since the latter point is attainable from the current loading point by an entirely elastic path, the elastic strain increment necessary to get from $N^l_{\alpha\beta}$ to $N^y_{\alpha\beta}$ is

$$\Delta\varepsilon_{\alpha\beta} = C^{-1}_{\alpha\beta\gamma\delta}\,\Delta N_{\gamma\delta}.$$

The axial stress increment in the ith family filaments is then

$$\Delta\sigma_i = E_i n^{(i)}_\alpha n^{(i)}_\beta C^{-1}_{\alpha\beta\gamma\delta}\,\Delta N_{\gamma\delta}.$$

When the ith family filaments are at either of the current yield stresses in tension σ^{tl}_i or compression σ^{cl}_i (equal to initial yield stresses only if there is no hardening), continued yielding will occur. Hence, if σ^l_i is the current stress in the ith family when $N_{\alpha\beta} = N^l_{\alpha\beta}$,

$$E_i n^{(i)}_\alpha n^{(i)}_\beta C^{-1}_{\alpha\beta\gamma\delta}(N^y_{\gamma\delta} - N^l_{\gamma\delta}) = \sigma^{tl}_i - \sigma^l_i,\ \sigma^l_i - \sigma^{cl}_i. \tag{10}$$

Equation (10) represents a pair of parallel plane surfaces in membrane stress space for the membrane stress $N^y_{\alpha\beta}$ which causes yield in the ith family. The interior intersection of all planes as $i = 1 \to m$ will constitute the current subsequent yield surface. As with initial yield and fracture surfaces, subsequent yield surfaces will be polyhedra of at most 2-m faces, and generally less than 2-m faces for $m > 3$ and substantial plastic yielding. Therefore, subsequent yield surfaces are also in general anisotropic.

It is noted that, by virtue of the assumed material behavior which is stable in Drucker's sense [6], the plastic strain increment is normal to the yield surface for stresses on a planar surface, and within the fan of normals at a corner or plane intersection. This may be demonstrated directly by use of equations (9 and 10).

Since the yield behavior of filamentary materials is described by a series of plane loading surfaces, the general results of Sanders [7] are applicable. In the present case, the plane loading surfaces (10) are not independent, but are dependent on one another through equation (3). Among other results, Sanders shows that final strains will be identical for all loading paths which produce the same final yield surface (see, also, [8]). This will always occur if loading paths continuously engage the same individual planes, and may occur if unloading takes place from one or more planes as long as the final positions of the planes for different load paths are identical. For loading paths of this nature, therefore, a deformation theory of plasticity will be valid. Examples illustrating this behavior are given below.

Example 1. *Three family material*

The socalled isotropic" filamentary array used in many important applications consists of three identical filament families at 60° to each other, as typified by the array in Fig. 6 where $\theta_i = 0°, \pm 60°$. For purposes of exposition, filament properties will be assumed identical in tension and compression. The initial yield surface for this material (identical to the fracture surface in Fig. 3 and also shown in Fig. 6a) is composed of 6 planar surfaces and deviates markedly from isotropic behavior (Fig. 4a).

If filaments are perfectly plastic ($E^T_i = 0$), this yield surface remains fixed under plastic action, and subsequent, initial yield, and limit [2] surfaces are the same. Stress–strain relations will be linear elastic and given by equations (4 and 5) when stresses are inside or unloading from the yield surface. Loading outside the yield surface is impossible, and continued plastic straining will produce the flat-topped stress–strain curve typical of perfectly plastic materials.

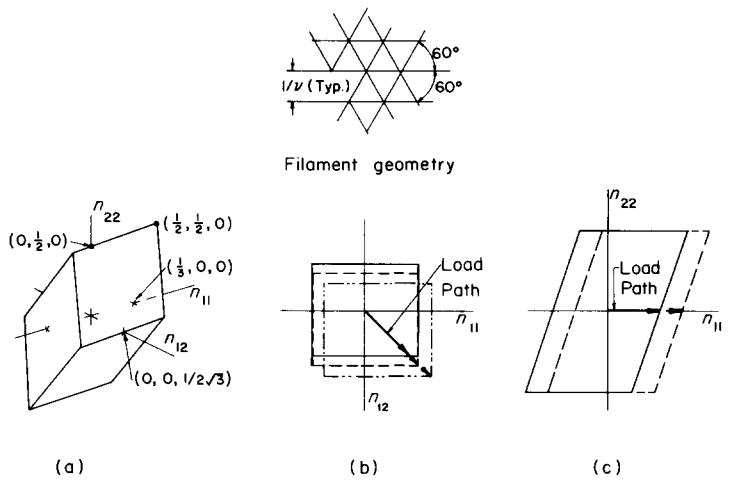

FIG. 6. Plastic behavior of $m = 3$, $\theta_i = 0, \pm 60°$ material. (a) Initial yield surface. (b) Subsequent yield surfaces under proportional loading in tension-shear. (c) Subsequent yield surfaces under simple tension for kinematic hardening filaments, $E^T/E = 1/20$. $n_{ij} = N_{ij}/3Av\sigma^{T0}$

When E_i^T = constant and filaments work-harden kinematically, the yield surface translates but does not change shape giving a type of kinematic hardening behavior for the composite (Figs. 6a, b, c). Note that this is not the kinematic hardening behavior described by Prager [9] whose model can be generalized to three dimensions as a smooth spherical ball which follows the loading path, pushing on the inside of a smooth yield surface. Prager's surface is free to translate in a direction normal to its boundary at the point of contact of the ball. While the filamentary material exhibits this behavior in tension–shear (Fig. 6b), its yield surface motion is not normal to the surface in simple tension (Fig. 6c). Neither a perfectly smooth nor a perfectly rough ball and surface can model this behavior.

Example 2. Four family material

The four family filamentary material in Fig. 7 has filaments at $\theta = 0, 90, \pm 45°$. If filament behavior is elastic–perfectly plastic, a limit surface [2] exists representing combinations of membrane stresses under which unlimited plastic flow can occur at constant load. For comparative purposes, the limit surface (dashed line) for the four family material is shown in Fig. 7a with the initial yield surface (solid line) for equal properties in tension and compression. The two surfaces coincide only in equal biaxial stress or pure shear corresponding to all filament families yielding simultaneously in tension or compression. Loading in simple tension along the N_{11} axis past initial yield to the limit surface and holding N_{11} constant while increasing N_{22} to its maximum value produces subsequent yield surfaces in the N_{11}–N_{22} plane as shown in Fig. 7b. Note that the yield surface both translates and significantly alters its shape as plastic loading progresses past initial yield. Also, the yield surface is never tangent to the limit surface and always has a vertex or corner touching the limit surface when the current loading state is at limit.

Nonproportional loading in tension and shear (N_{11}–N_{12} plane) for kinematic work-hardening filaments with E_i^T = constant is shown in Fig. 7c. For the three load paths

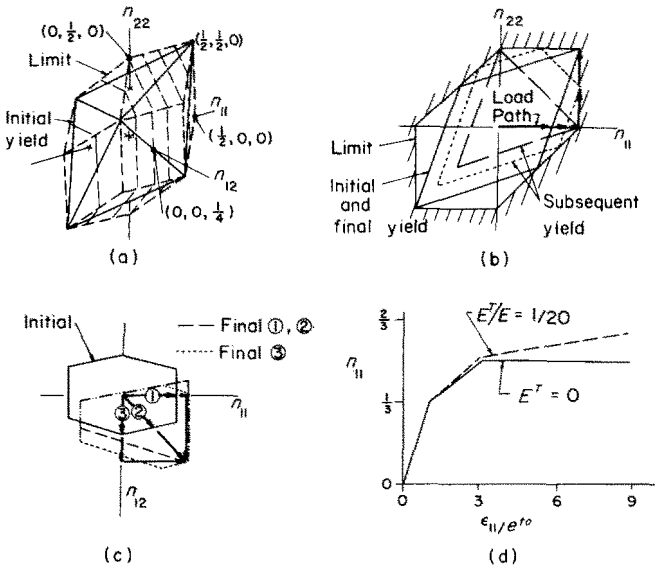

FIG. 7. Plastic behavior of $m = 4$, $\theta_i = 0, \pm 45, 90°$ material. (a) Initial yield and limit surfaces. (b) Subsequent yield surfaces under non-proportional biaxial loading, $E^T = 0$. (c) Subsequent yield surfaces under proportional and non-proportional loading in tension-shear, kinematic hardening filaments, $E^T/E = 1/20$. (d) Stress–strain curves in simple tension $n_{ij} = N_{ij}/4Av\sigma^{t0}$.

shown, all ending at the same stress point, proportional loading ($N_{11} = N_{12}$) and tension-then-shear (N_{11}, N_{12}) produce the same final yield surface and total strains. Shear-then-tension loading gives a different yield surface and strains. The proportional and tension-then-shear loadings both cause motion of the same loading faces, and unloading from a plastic state never occurs in a filament family. Under these conditions, a deformation theory of plasticity will be applicable as discussed previously. These conditions do not hold, however, for the shear-then-tension loading where the filaments at $\theta = -45°$ are given a significant plastic strain during the shear loading, then unloaded during the end of the tensile phase as the filaments at $\theta = 0°$ begin to yield in tension. Hence, the deformation theory is not applicable to the latter loading.

Stress–strain behavior in simple tension for this material is shown in Fig. 7d. For perfectly plastic filaments, the material is macroscopically linear work hardening from initial yield to the limiting state, then perfectly plastic. In the case of kinematic linear work-hardening filaments, stress strain behavior is bilinear work hardening.

Example 3. *Infinite family uniformly oriented material*

As the number m of equiangularly oriented families becomes large and cross-sectional area A_i becomes small such that $\sum_{i=1}^{m} A_i v_i$ remains constant, the filamentary material approaches a continuous, uniformly oriented array which is initially plastically isotropic as well as elastically isotropic. Once loading progresses past initial yield, however, yield behavior becomes anisotropic. For perfectly plastic filaments, Fig. 8a shows the change in shape of the yield surface for loading in simple tension from initial yield to the limit surface. Note that the yield surface collapses to a line at limit, and elastic behavior occurs only upon unloading along the N_{11} axis. Typical behavior for kinematic linear work-hardening

filaments is illustrated in Fig. 8b for tension–shear loading. As with the four family material, tension-then-shear loading gives different yield behavior from shear-then-tension loading, but the difference is less pronounced. Stress–strain behavior in simple tension (Fig. 8c) shows that the material work-hardens asymptotically to perfectly plastic behavior for $E_i^T = 0$, and to linear work hardening for $E_i^T =$ constant.

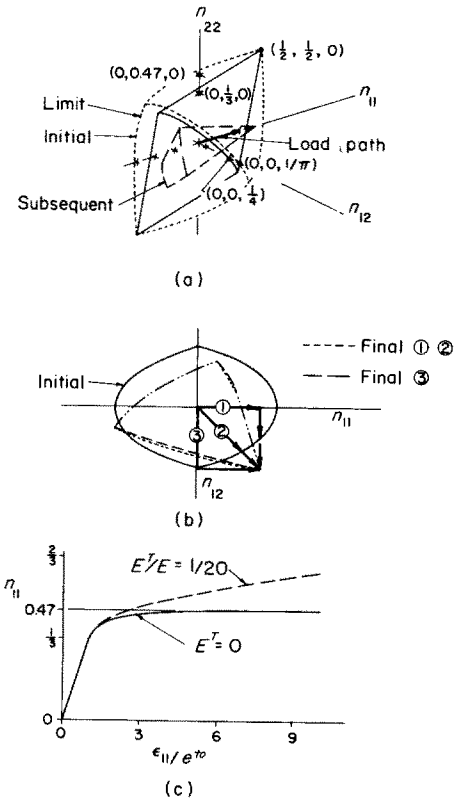

FIG. 8. Continuous, uniformly oriented ($m \to \infty$) material plastic behavior. (a) Initial yield, limit, and subsequent yield surfaces under simple tension loading, $E^T = 0$. (b) Subsequent yield surfaces under proportional tension-shear loading, $E^T/E = 1/20$. (c) Stress–strain curves in simple tension for perfectly plastic ($E_T = 0$) and work-hardening ($E_T/E = 1/20$) filaments. $n_{ij} = N_{ij}/\pi A \nu^\circ \sigma^{*0}$ where ν° is number of filaments per unit orientation angle θ.

CONCLUSIONS

The essential aspects of elastic, fracture and plastic behavior of filamentary materials with three or more filament families have been investigated by treating idealized planar arrays of filaments with general elastic–brittle or elastic–plastic behavior. Specific examples using elastic–brittle, elastic–perfectly plastic, and elastic–kinematic linear work hardening were computed using the program described in the Appendix to illustrate main points, but the method outlined herein can in principle be used for any filament behavior.

While the behavior of equiangular filamentary arrays with identical filament properties is elastically isotropic, fracture and yield behavior are generally anisotropic. As the number of equiangularly oriented filament families increases, initial yield and fracture properties more closely approach isotropy. Subsequent yield behavior, however, is anisotropic even

in the limiting case of an infinite number of filament families continuously distributed in the plane.

Under proportional loading, macroscopic stresses which cause fracture of the first filament family also represent the maximum stresses which can be carried by the filamentary material. Subsequent fracture surfaces lie inside the initial fracture surface except for a small range of loadings generally far away from the stress state which causes initial fracture. Therefore, initial fracture surfaces may for practical purposes be treated as failure surfaces for these elastic–brittle filamentary materials.

Subsequent plastic flow past initial yield is controlled by dependent plane loading surfaces which correspond to individual filament family behavior. For perfectly plastic and work-hardening behavior, yield surfaces both change their shape and translate as loading progresses for all filamentary arrays except $m = 3$. Hence, the usual kinematic or isotropic hardening models do not describe filamentary material behavior. Under certain loadings to the same stress state, yield surfaces and final strains are identical indicating that deformation theories may be used under restricted conditions. Plastic stress–strain behavior is macroscopically work-hardening, even while loading perfectly plastic filamentary arrays from initial yield to the limit surface.

Acknowledgement—The partial support of the National Science Foundation under grant GK-5582 while making this study is gratefully acknowledged. The authors are also grateful for computer time made available by the Graduate College, University of Illinois at Urbana-Champaign.

REFERENCES

[1] A. KELLY and G. J. DAVIES, The principles of the fibre reinforcement of metals. *Met. Rev.* **10**, 1–77 (1965); E. Z. STOWELL and T. S. LIU, On the mechanical behavior of fibrereinforced crystalline materials. *J. Mech. Phys. Solids*, **9**, 242–260 (1961).

[2] P. V. McLAUGHLIN, JR. and S. C. BATTERMAN, Limit behavior of fibrous materials. *Int. J. Solids Struct.* **6**, 1357–1376 (1970).

[3] P. V. McLAUGHLIN, JR., Plastic limit behavior and failure of filament reinforced materials. *Int. Solids Struct.* **8**, 1299–1318 (1972).

[4] C. WOZNIAK, Theory of fibrous media—I and II, *Arch. Mech. Stosowanej* **17**, 651–699: 777–799 (1965).

[5] P. V. McLAUGHLIN, JR. and S. C. BATTERMAN, On extending the range of applicability of the limit theorems. *J. appl. Mech.* **37**, 518–521 (1970).

[6] D. C. DRUCKER, A More fundamental approach to plastic stress–strain relations. *Proceedings of the 1st National Congress of Applied Mechanics. A.S.M.E.*, pp. 487–491, New York (1951); D. C. DRUCKER, On the postulate of stability of material in the mechanics of continua. *J. Mécanique* **3**, 235–249 (1964): D. C. DRUCKER, Plasticity. *Structural Mechanics*, pp. 407–455. Pergamon Press, Oxford (1960).

[7] J. L. SANDERS, JR., Plastic stress–strain relations based on linear loading functions. *Proceedings of the 2nd U.S. National Congress of Applied Mechanics, A.S.M.E.*, pp. 455–460, New York (1954).

[8] S. B. BATDORF and B. BUDIANSKY, Polyaxial stress–strain relations of a strain-hardening metal. *J. appl Mech.* **21**, 323–326 (1954).

[9] W. PRAGER, The theory of plasticity: A survey of recent achievements. (James Clayton Lecture). *Proceedings of the Institution of Mechanical Engineers* **169**, 41–57 (1955).

APPENDIX—NUMERICAL SOLUTION OF INCREMENTAL STRESS–STRAIN EQUATIONS AND GRAPHICAL PRESENTATION OF YIELD AND FRACTURE SURFACES

Calculation of stress–strain histories

If the macroscopic *strain* increment of a filamentary material is specified, the stress increment is computed directly (through incremental equations (1, 8 and 9) in the main

body of the paper) from knowing the axial strain increment in each filament. However, if the macroscopic *stress* increment is specified, an iterative procedure for determining incremental macroscopic strains at each stage of loading is required. Filaments are initially assumed to remain elastic and the macroscopic strain increment is computed from equation (9c) with $D_{\alpha\beta\gamma\delta} \equiv 0$. The axial strain in each filament family is then computed through equation (1) and filaments that have yielded are identified. The Young's moduli for yielded filaments are then replaced by secant moduli corresponding to their respective calculated axial strains. These secant moduli are then used in place of the Young's moduli to construct a corrected value of $C_{\alpha\beta\gamma\delta}$ in equation (4c). The whole procedure is repeated until a desired accuracy is achieved. At each step of loading, filament stresses and strains are stored for subsequent computations.

Computer construction of yield and fracture surfaces

In the graphics computer program, a basic subroutine "hit" determines the intersection of the yield or fracture surface with a directed line segment passing through a given base point known to be inside the surface. The subroutine first determines the base strains in all filaments associated with the given interior point, and computes the changes in axial strains associated with the specified direction. Then for each filament, the difference between the relevant critical strain and the base strain is divided by the change in strain; the smallest such quotient is multiplied by the direction vector and the result is used to compute, through equations (1, 8 and 9), the change in stress necessary to reach the yield or fracture surface. This stress increment is then added to the stress base point to get the required intersection.

By calls to subroutine "hit", a higher-level subroutine "locus" determines the corners of the polygonal intersection of the yield or fracture surface with a plane passing through a given base point and having a specified normal direction. Intersections of current yield surfaces with coordinate planes are obtained by letting the base point be the origin and by letting the normal direction coincide with the 11, 22 and 12 axes in turn.

The actual polyhedral yield surface is constructed in an axonometric view by considering each of the possible 2-m faces in turn. The normal direction to each face is determined and a point in the face is found. Subroutine "locus" then locates the corners of the face. In plotting the yield surfaces, an axonometric transformation of face corner point coordinates is effected and lines are drawn between them.

(*Received* 6 *September* 1972; *revised* 2 *February* 1973)

Абстракт—Исследуются характерные свойства упругого поведения, хрупкого разрушения и пластического течения для материалов, составленных из решеток упруго-хрупких или упруго-пластических волокон, под влиянием плоского напряженного состояния. Определяются линейные упругие конститутивные зависимости для нитеобразного материала и исследуются условия плоской упругой изотропии. Для хрупких материалов с волокнами вычисляются начальные и последующие поверхности разрушения/которые вообще анизотропны/и поведение напряжение-дефориация. Даются выражения для законов постепенно нарастающего пластического напряжения и деформации, начальных поверхностей течения и последующих поверхностей пластичности, для обшего случая механического упрочнения волокон. Приводятся примеры для хрупких и идеально пластических волокон и для волокон с кинематическим линейным механическим упрочнением. Они иллюстрируют использование анализа и главные результаты.